

DERIVING THE MACROCONTACT CONDITION BETWEEN CEMENTLESS HIP REPLACEMENT AND BONE FROM THE MICROGEOMETRY OF THE REPLACEMENT COATING

Julia Orlik¹, Alexei Zhurov², and John Middleton³

ABSTRACT

We consider mature femoral cortical bone which is in contact with a hip implant having a rough coating. The bone is assumed to be separated from the implant by a thin layer of microscopic peaks and valleys formed on the surface of the coating. The size of the peaks and valleys is very small compared with the macroscale of the implant stem and bone. This makes the direct application of the FEM for the calculation of the bone–stem contact problem prohibitively costly. A method is developed that allows deriving a macrocontact condition on the bone–stem interface. The method involves an asymptotic homogenisation procedure that takes into account the microgeometry of the interface layer and the stiffnesses of the bone and the implant material. The macrocontact condition is then used in a FEM model for the bone–stem contact problem on the macroscale. The averaged contact stiffness obtained allows the replacement of the interface layer in the macromodel by the macrocontact condition. An approximation to the microstresses is found by two-scale homogenization and can be used for the macrostrength estimation.

1. INTRODUCTION

Treatment for hip osteoarthritis focuses on decreasing pain and improving joint movement. When conservative methods of treatment fail, it is necessary to replace the affected joint with an artificial replacement called a joint prosthesis. Nowadays there are two types of hip prosthesis: cemented and cementless. The cementless hip prosthesis, the most recent type, represents approximately 35% of the European market and is regarded as more promising. The surface of the cementless implant is coated in such a way that the bone is in direct contact with this surface with the idea that the bone grows into the microvalleys and pores of the coating to provide enhanced stability and rapid osseointegration.

The aim of the present paper is to investigate the dependence of the bone–implant contact condition on the microgeometry and mechanical properties of the coating. To achieve

Keywords: asymptotic homogenisation, contact problems, bone-implant interaction

¹ Research Fellow, Fraunhofer Institut Techno- und Wirtschaftsmathematik, Kaiserslautern, Germany

² Research Assistant, UWCM, Biomechanics Research Unit, Cardiff Medicentre, Cardiff CF14 4UJ, UK

³ Reader, UWCM, Biomechanics Research Unit, Cardiff Medicentre, Cardiff CF14 4UJ, UK

this aim, we develop an asymptotic homogenisation procedure based on the results of [1–2] and extend the approach of [3–5] to elastic contact problems.

We assume that the contact areas are known, thus confining ourselves to linear problems. From the mechanical point of view, the contact zones are known only if the micro-peaks (punches) either have plane summits and equal heights (e.g., are parallelepipeds or cylinders) or have arbitrary geometry but all free space is filled by bone (i.e., the bone is in ideal contact with the implant).

We make the following assumptions: (i) the problem is linearly elastic; (ii) the micro-contact surfaces are known, and consequently, the problem is linear; (iii) either there is no friction or Coulomb’s friction law is adopted, and hence, the shear stresses at the contact boundary are either zero or proportional to the normal stress; (iv) the bone and implant materials are assumed homogeneous; and (v) there is a small parameter, ε , the ratio of the characteristic dimension of the interface irregularities to the characteristic length of the bone–implant interaction zone, which allows applying an asymptotic homogenisation procedure.

2. MATHEMATICAL STATEMENT OF THE MICROCONTACT PROBLEM

We consider two contacting domains, D^ε (implant) and Ω^ε (bone), as schematically shown in Fig. 1. The right part of the boundary of D^ε is assumed to have a pattern represented by identical peaks with plane summits arranged periodically with period εY_0 , where ε is a small parameter and Y_0 is a characteristic length of the interaction zone. The domain Ω^ε is in contact with D^ε at the summits. Formally we assume that Ω^ε is a Lipschitz domain in the n -dimensional Euclidean space; in applications $n = 2$ or 3 but our reasoning and relations obtained below will be valid for any n . We introduce also a fixed domain $\Omega \subset \Omega^\varepsilon$ such that $\Omega^\varepsilon \setminus \Omega \subset \Pi^\varepsilon$, where Π^ε is the thin layer containing the peaks of D^ε (Fig. 1); the measure of $\Omega^\varepsilon \setminus \Omega$ tends to zero as $\varepsilon \rightarrow 0$.

Let $x = (x_1, \dots, x_n)$ and $\hat{x} = (x_2, \dots, x_n)$ be the coordinates of a point in \mathbb{R}^n and those of a point at the contact interface, the hyperplane $x_1 = 0$. The microcontact surface will be defined by $S_C^\varepsilon = \{x \in \mathbb{R}^n : \hat{x} \in S_0 \cap \text{Proj}_{\{x_1=0\}}(\varepsilon S_C), x_1 = \varepsilon F(\hat{x}, \frac{\hat{x}}{\varepsilon})\}$, where the macrocontact surface $S_0 = \bar{\Omega} \cap \{x : x_1 = 0\} \setminus \partial\Omega_N$ and F is a Lipschitz function Y_0 -periodic in \hat{x} . Furthermore, for the periodicity cell, we introduce the local coordinates ξ that are related to x by $x = \varepsilon\xi$ and denote by T the cross section of the periodicity cell by a hyperplane $\xi_1 = \text{const}$, i.e., $T = \{\xi : 0 < \xi_j < Y_0, j = 2, \dots, n\}$. The other notation should be clear from Fig. 1.

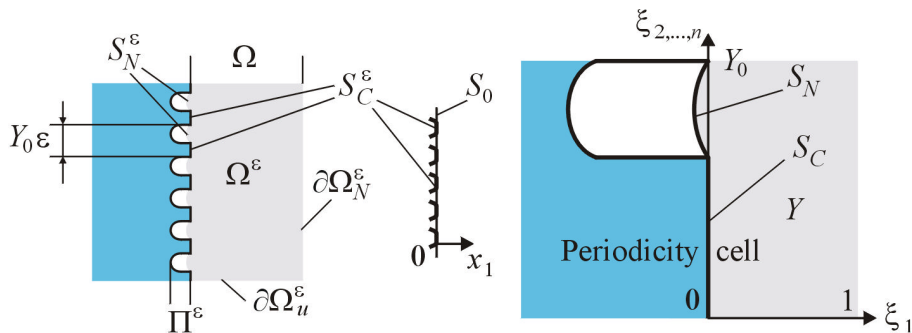


Figure 1: Contact domains and some notation

We consider the case where the domains are bounded and periodic boundary (contact) conditions are imposed. For the elastic bone occupying the domain Ω^ε , denote by $(\sigma_{ij}^\varepsilon(x))_{n \times n}$ the stress tensor, $(u_i^\varepsilon(x))_n$ the displacement vector, and $(a_{ijkl}(x))$ the n -dimensional symmetric 4-order tensor of elastic constants at a point $x \in \Omega^\varepsilon$.

We write out the equilibrium equations and constitutive elastic relations with contact and boundary conditions:

$$\frac{\partial \sigma_{ij}^\varepsilon(x)}{\partial x_j} = f_i(x), \quad \sigma_{ij}^\varepsilon(x) = a_{ijkl} \frac{\partial u_k^\varepsilon(x)}{\partial x_l}, \quad x \in \Omega^\varepsilon, \quad (1)$$

$$\sigma_n^\varepsilon(x) = b\left(\hat{x}, \frac{x}{\varepsilon}\right) [u_n^\varepsilon(x)], \quad \sigma_{it}^\varepsilon(x) = \mu \sigma_n^\varepsilon(x) \frac{u_{it}^\varepsilon}{|u^\varepsilon|}, \quad x \in S_C^\varepsilon, \quad (2)$$

$$\sigma_{ij}^\varepsilon n_j(x) = 0, \quad x \in S_N^\varepsilon \cup \partial\Omega_N^\varepsilon; \quad u_i^\varepsilon(x) = 0, \quad x \in \partial\Omega_u^\varepsilon. \quad (3)$$

Here, $\sigma_n^\varepsilon(x) = \sigma_{ij}^\varepsilon(x) n_j(x) n_i(x)$ is the normal stress, $\sigma_{it}^\varepsilon(x) = \sigma_{ij}^\varepsilon(x) n_j(x) - \sigma_n^\varepsilon n_i(x)$ are the components of the tangential stress vector, $u_n^\varepsilon(x) = u_i^\varepsilon(x) n_i(x)$ is the normal displacement, $u_{it}^\varepsilon(x) = u_i^\varepsilon(x) - u_n^\varepsilon n_i(x)$ are the tangential displacements, $n_i(x)$ are the components of the unit normal to the contact interface, and μ is the friction coefficient ($\mu = 0$ in the case of pure sliding). The Latin subscripts assume the values from 1 to n .

Relations (1)–(3) represent the strong formulation of the problem, which applies to smooth domains as well as smooth elastic coefficients and right-hand-side functions (prescribed volume forces, boundary displacements, and tractions). Since we deal with non-smooth domains and allow nonsmooth functions and intend to adopt the finite element method for numerical solution, we rewrite the problem in a weak (variational) formulation.

For any test function $v_i \in H^1(\Omega^\varepsilon, \partial\Omega_u^\varepsilon)$, the solution $(u_i^\varepsilon)_n$ of problem (1)–(3) must satisfy the following variational equation:

$$\begin{aligned} \int_{\Omega^\varepsilon} a_{ijkl} \frac{\partial u_k^\varepsilon(x)}{\partial x_l} \frac{\partial v_i(x)}{\partial x_j} dx + \int_{S_C^\varepsilon} b\left(\hat{x}, \frac{x}{\varepsilon}\right) u_n^\varepsilon(x) v_n ds \\ + \int_{S_C^\varepsilon} \mu b\left(\hat{x}, \frac{x}{\varepsilon}\right) u_n^\varepsilon(x) \frac{u_{it}^\varepsilon}{|u^\varepsilon|} v_{it}(x) ds = \int_{\Omega^\varepsilon} f_i(x) v_i(x) dx. \end{aligned} \quad (4)$$

3. HOMOGENISATION PROCEDURE AND BASIC RESULTS

Since problem (1)–(3), as well as its variational formulation (4), has two different size scales on the micro- and macrolevels, it is very difficult to perform its direct numerical solution. So we intend to reduce the problem to a single-scale problem and then numerically solve it. For the scale reduction, asymptotic homogenisation was chosen.

We perform the following stages: (i) determine the averaged contact conditions, which will then be used to replace the contact layer, (ii) calculate the macrodisplacements and stresses in the domain Ω with the averaged boundary conditions obtained, (iii) find an approximation to the microstresses in the boundary layer by a formal asymptotic expansion, and (iv) insert this approximation into some microstrength condition to predict if fracture can occur somewhere in the bone under the applied loading.

In equation (4), we pass to the limit as $\varepsilon \rightarrow 0$ in accordance with the two-scale homogenisation procedure to obtain for any $v_i^0 \in H^1(\Omega, \partial\Omega_u)$ the following relation:

$$\begin{aligned} \int_{\Omega} a_{ijkl} \frac{\partial u_k^0(x)}{\partial x_l} \frac{\partial v_i^0(x)}{\partial x_j} dx + \frac{1}{|T|} \int_{S_0} \left(\int_{S_C} b(\hat{x}, \xi) u_n^0(0, \hat{x}) ds_\xi \right) v_n^0(0, \hat{x}) d\hat{x} \\ + \frac{1}{|T|} \int_{S_0} \left(\int_{S_C} \mu b(\hat{x}, \xi) u_n^0(0, \hat{x}) ds_\xi \right) \frac{u_{it}^0}{|u^0|} v_{it}^0(0, \hat{x}) d\hat{x} = \int_{\Omega} f_i(x) v_i^0(x) dx, \end{aligned} \quad (5)$$

where $|T|$ stands for the measure of the domain T . For details, see Theorem 3 in [3] and Lemma 5.4 in [2], for the convergence of the surface integrals.

To the variational formulation (5) there corresponds the *homogenized problem* in the strong formulation

$$\frac{\partial \sigma_{ij}^0(x)}{\partial x_j} = f_i(x), \quad \sigma_{ij}^0(x) = a_{ijkl} \frac{\partial u_k^0(x)}{\partial x_l}, \quad x \in \Omega, \quad (6)$$

$$\sigma_n^0(x) = B(\hat{x})[u_n^0(x)], \quad \sigma_{it}^0(x) = \mu \sigma_n^0(x) \frac{u_{it}^0}{|u^0|}, \quad x \in S_0, \quad (7)$$

$$\sigma_{ij}^0(x) n_j(x) = 0, \quad x \in \partial\Omega_N; \quad u_i^0(x) = 0, \quad x \in \partial\Omega_u. \quad (8)$$

Carrying out calculations, we arrive at the main result, the homogenized normal contact stiffness. We have

$$B(\hat{x}) = \frac{1}{|T|} \int_{S_C} b(\hat{x}, \xi) ds_\xi \equiv \frac{1}{|T|} \int_{\text{Proj}_{\{\xi_1=0\}}(S_C)} b(\hat{x}, \hat{\xi}) \sqrt{1 + [\nabla_\xi F(\hat{x}, \hat{\xi})]^2} d\hat{\xi} \quad (9)$$

From the mechanical literature we know that $b = \text{const}$ for Winkler's base and $b = \frac{2E}{1-\nu^2} (x_2^2 + \dots + x_n^2)^{1/4}$ for the Hertzian base. As an example, we take $b = \text{const}$, $\mathbb{R}^n = \mathbb{R}^3$, and derive the effective contact stiffness B for two cases of the interface microgeometry:

(i) $F \equiv 0$ (system of plane punches). Let the punches be identical cylinders of radius a^ε or parallelepipeds of square cross-section with side a^ε . Then formula (9) yields

$$\boxed{B = b |S_C| / Y_0^2, \text{ where } |S_C| = \pi a^2 \text{ or } a^2, a = \varepsilon^{-1} a^\varepsilon < Y_0.} \quad (10)$$

(ii) $F(\hat{\xi}) = \sqrt{a^2 - \xi_2^2 - \xi_3^2}$ (system of hemispheres of radius a^ε). According to our assumption, we consider the full contact; otherwise the contact surface is unknown and the problem becomes nonlinear. Formula (9) gives

$$\boxed{B = b [1 + \pi (a/Y_0)^2].}$$

Whenever a solution $u_i^0(x)$ of problem (6)–(8) is found, which is a homogenised macrosolution, we can obtain a corresponding microsolution by asymptotic expansion. The microsolution will serve to identify fracture regions.

Let εY be the period of the structure at the interface. We look for a microsolution $u_i^\varepsilon(x)$ in the form of an asymptotic expansion [3]:

$$u_i^\varepsilon(x) = \begin{cases} u_i^0(x) & \text{if } x \in \Omega, \\ u_i^0(x) + \varepsilon \Theta_{ip}(\xi) u_p^0(x) + \varepsilon N_{pqi}(\xi) \frac{\partial u_q^0(x)}{\partial x_p} + O(\varepsilon^2) & \text{if } x \in \Pi^\varepsilon, \end{cases}$$

where $\xi = x/\varepsilon$, $x \in \Omega$, $\xi \in Y$, and $\Pi^\varepsilon = \Omega^\varepsilon \cap \{x : 0 < x_1 < Y\varepsilon\}$. Here, $(u_i^0)_n$ is the solution of macroproblem (6) obtained after replacing the contact layer by the homogenized contact condition (7) with the new normal contact stiffness defined by (9), and $(\Theta_p)_{n \times n}$ and $(N_{pqk})_{n \times n \times n}$ are periodic solutions of auxiliary problems for the periodicity cell, which are not written out here.

The following approximation to the microstresses in the contact layer Π^ε can be derived formally as

$$\begin{aligned} \sigma_{ij}^\varepsilon(x, \xi) &= a_{ijkl} \frac{\partial \Theta_{kp}(\xi)}{\partial \xi_l} u_p^0(x) + a_{ijkl} \frac{\partial}{\partial \xi_l} (N_{pqk}(\xi) + \xi_p \delta_{qk}) \frac{\partial u_q^0(x)}{\partial x_p} \\ &+ \varepsilon \left[a_{ijkl} \Theta_{kp}(\xi) \frac{\partial u_p^0(x)}{\partial x_l} + a_{ijkl} N_{pqk}(\xi) \frac{\partial^2 u_q^0(x)}{\partial x_p \partial x_l} \right] + O(\varepsilon^2). \end{aligned} \quad (11)$$

To predict the appearance of fracture regions, we need to use one or another *strength condition* for the ε -problem (1)–(3):

$$\sup_{x \in \Omega^\varepsilon} \sigma_{\text{eq}}(\sigma_{ij}^\varepsilon(x, \xi)) < \sigma_u. \quad (12)$$

Here σ_u is the ultimate stress for the bone, and σ_{eq} is the equivalent stress, which can be chosen in accordance with one of the familiar strength conditions (von Mises or Tresca):

$$\sigma_{\text{eq}}(\sigma_{ij}(x)) = \sqrt{\frac{3}{2}s_{kl}(x)s_{kl}(x)}, \quad \sigma_{\text{eq}}(\sigma_{ij}(x)) = \max_{k,l=1,\dots,3} |\sigma_k(x) - \sigma_l(x)|, \quad (13)$$

where $s_{ij} = \sigma_{ij} - \frac{1}{3}\delta_{ij}\sigma_{kk}$. It can be proved that the *macrostrength condition for the contact layer* becomes

$$\sup_{\hat{x} \in S_0} \sup_{\xi \in Y} \sigma_{\text{eq}}(\sigma_{ij}^0(x, \xi)) < \sigma_u, \quad (14)$$

where $\sigma_{ij}^0(x, \xi) = \sigma_{ij}^\varepsilon(x, \xi)|_{\varepsilon=0}$. From the practical point of view this means that as soon as solutions of problem (6–8) and the problems for Θ_p and N_{pqk} are found, the macrostrength in the boundary layer can be estimated by the last relation.

4. NUMERICAL SOLUTION

In computations, the finite element software package ANSYS was used. The materials of the implant and bone were assumed homogeneous and isotropic with Young's moduli $E_{\text{impl}} = 100$ GPa and $E_{\text{bone}} = 9$ GPa, Poisson's ratios $\nu_{\text{impl}} = 0.30$ GPa and $\nu_{\text{bone}} = 0.27$ GPa, friction coefficient $\mu = 0.3$, and normal contact stiffness $b = 200$ GPa.

First we considered the microcontact problem for Θ_p for a unit cell. The geometry of contact regions is depicted in Fig. 2 and the contact, boundary, and symmetry conditions are shown in Fig. 3. The implant coating hills were taken to be rectangular parallelepipeds square in plan with side $a = 0.4$ (here a is dimensionless but typically it ranges between 5 and 500 μm). Due to symmetry, only one eighth of the unit cell was studied. The corresponding distribution of von Mises stresses is presented in Fig. 4.

Further we considered a macrocontact problem for the axisymmetric bone–implant system shown in Fig. 5. The femur bone is modelled by a hollow cylinder fully clamped at the base. The implant is modelled by a solid cylinder whose lower part has the shape of a frustum of a cone. The radius of the upper part of the cylinder slightly exceeds the interior radius of the bone, which means that the implant tightly fits into the bone and the structure is in a prestrained state. The dimensions are shown in Fig. 5. A pressure of 1 MPa is applied to the top end of the implant, which approximately corresponds to half the weight of a patient. By formula (10) we have $B = (a^2/Y_0^2)b = 32$ GPa for the homogenized normal contact stiffness.

Figures 6(a)–(d) depict the computation results for the macrocontact problem under consideration. The axial stress field has regions of increased stresses near the points where the implant detaches from the bone. These are corner points, where the stem geometry changes from cylindrical to conical, and points of change of boundary conditions. Mathematically, stress singularities can occur at such points. As one should expect, the maximal equivalent stresses arise near the contact interface.

REFERENCES

1. Hansson, S. and Norton, M., The relation between surface roughness and interfacial shear strength for bone-anchored implants. A mathematical model, J. Biomech., 1999, Vol. 32, 829–36
2. Yosifian, G. A., Some Unilateral Boundary Value Problems for Elastic Bodies with Rugged Boundaries, Preprint 99-18 (SFB 359), Heidelberg, 1999
3. Jäger, W., Oleinik, O. A., and Shaposhnikova, T. A., Homogenization of solutions of the Poisson equation in a domain perforated along a hypersurface, with mixed boundary conditions on the boundary of the cavities, Trans. Moscow Math. Soc., 1998, Vol. 59, 135–57
4. Jäger, W., Oleinik, O. A., and Shaposhnikova, T. A., On homogenization of solutions of the Poisson equation in a perforated domain with different types of boundary conditions on different cavities, Applicable Analysis, 1997, Vol. 65, 205–23
5. Belyaev, A. G., Piatnitski, A. L., and Chechkin, G. A., Asymptotic behaviour of a solution to a boundary value problem in a perforated domain with oscillating boundary, Sib. Math. J., 1998, Vol. 39, No. 4, 621–44

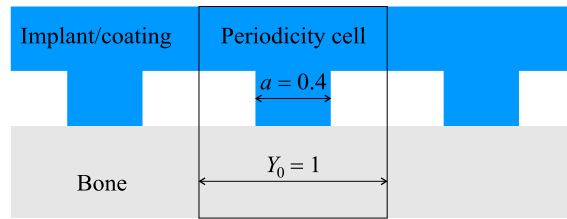


Figure 2: Microgeometry of contact domains

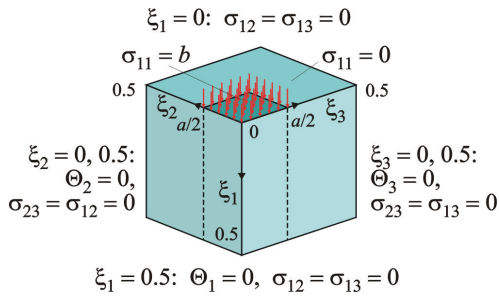


Figure 3: One eighth of the periodicity cell. Boundary conditions for the Θ_p -problem

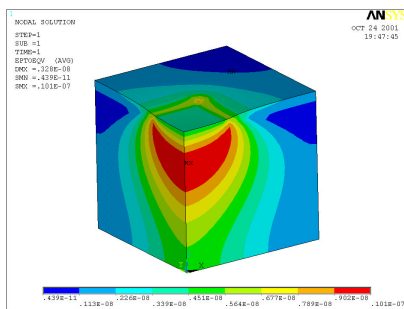


Figure 4: Von Mises equivalent stress in the periodicity cell, $\tilde{\sigma}_{eq}(\Theta_p(\xi))$

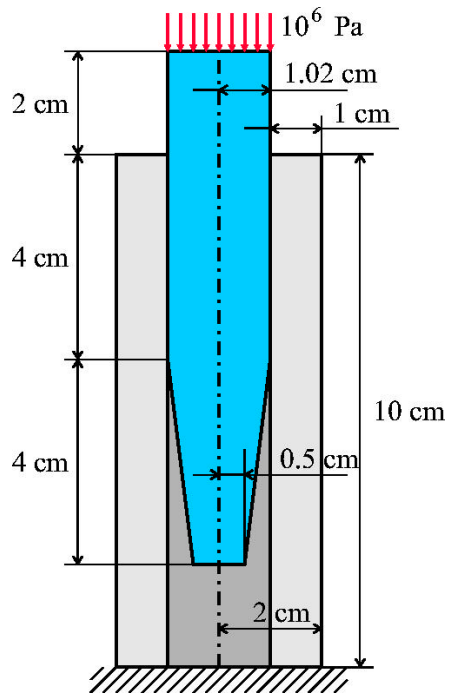


Figure 5: Macrocontact of a bone with a hip prosthesis

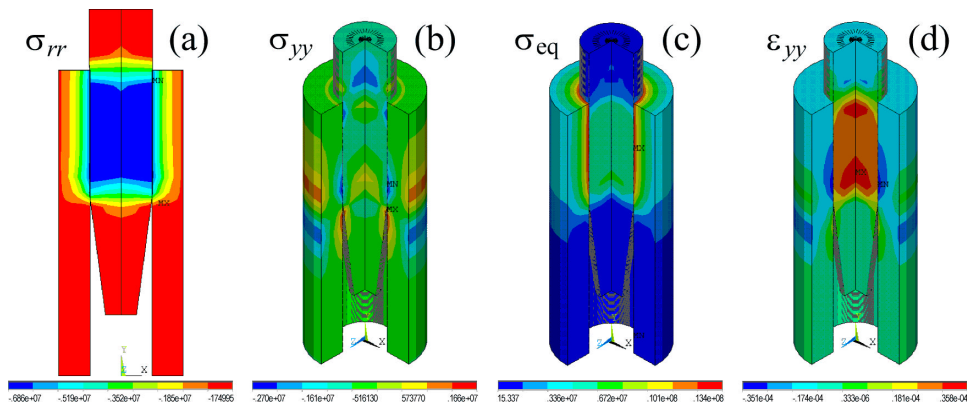


Figure 6: Stress and strain distributions in the macrocontact problem: (a) radial stresses (frontal view), (b) axial stresses (isometric view), (c) equivalent von Mises stresses, and (d) equivalent von Mises strains